



HAL
open science

Prediction of Aging Impact on Electromagnetic Susceptibility of an Operational Amplifier

He Huang, Alexandre Boyer, Sonia Ben Dhia, Bertrand Vrignon

► **To cite this version:**

He Huang, Alexandre Boyer, Sonia Ben Dhia, Bertrand Vrignon. Prediction of Aging Impact on Electromagnetic Susceptibility of an Operational Amplifier. Asia-Pacific International EMC Symposium 2015, May 2015, Taipei, Taiwan. 4p. hal-01159222

HAL Id: hal-01159222

<https://hal.science/hal-01159222>

Submitted on 5 Jun 2015

HAL is a multi-disciplinary open access archive for the deposit and dissemination of scientific research documents, whether they are published or not. The documents may come from teaching and research institutions in France or abroad, or from public or private research centers.

L'archive ouverte pluridisciplinaire **HAL**, est destinée au dépôt et à la diffusion de documents scientifiques de niveau recherche, publiés ou non, émanant des établissements d'enseignement et de recherche français ou étrangers, des laboratoires publics ou privés.

Prediction of Aging Impact on Electromagnetic Susceptibility of an Operational Amplifier

He HUANG^{#*1}, Alexandre Boyer^{#*2}, Sonia Ben Dhia^{#*3}, Bertrand Vrignon⁺⁴

[#]CNRS, LAAS, 7 avenue du colonel Roche, F-31400 Toulouse, France

^{*}Univ de Toulouse, INSA, LAAS, F-31400 Toulouse, France

¹he.huang@laas.fr

²alexandre.boyer@laas.fr

³sonia.bendhia@laas.fr

⁺Analog & Sensor group, Freescale Semiconductor, Inc.

134 av. Du Général Eisenhower, 31023 Toulouse, France

⁴bertrand.vrignon@freescale.com

Abstract—This paper deals with the impact of aging on the electromagnetic susceptibility level of a CMOS operational amplifier (opamp). The aging impact can be modelled by the variation of several parameters of the MOSFET model, to predict the evolution of electromagnetic susceptibility (EMS) of the opamp block during the aging process.

I. INTRODUCTION

The increasing use of high speed and complex electronic systems makes the electromagnetic compatibility (EMC) an important issue for the electronic manufacturers [1]. Some experimental results show the significant reduced EMC evolution after aging stress [2]. Thus how to ensure EMC during the whole lifetime of IC products, which is called electromagnetic robustness (EMR), becomes a new study in the recent years.

As presented in only few works, the simulation can be used to predict the long-term EMC behaviour. For example, in [3], the increase of the electromagnetic emission of a DC-DC converter after thermal stress is modeled, which is associated to the degradation of filtering passive devices. In [4], the simulation results confirm the evolution of the EMS of a phase-locked loop (PLL) before and after aging. The aging affects the threshold voltage and the mobility of the MOSFET of the PLL. However, in these case studies only two statuses (the device before and after a period of aging) are measured and simulated. Thus there is a lack of more precise insight about the evolution of the different phases during the whole aging time.

As a common electronic block, the operational amplifier is very susceptible to the external electromagnetic interference (EMI). The coupling of EMI on opamp inputs and power supply leads to a distortion of the output voltage, especially the generation of a voltage offset on its output which is harmful and hard to remove [5], [6]. In this study, with the aging stress injected in several parts of the amplifier, a worse DC output offset value at several frequencies could be observed, that means the device becomes more susceptible to the EMI with the aging. So the prediction of EMS evolution becomes important to help the IC designers to prevent EMC failure during the ICs' lifetime.

This paper aims at demonstrating through a case study the impact of aging on electromagnetic susceptibility of an operational amplifier, and the prediction method of the aging impact. Section II presents briefly the experimental set-up and the aging process. The measurement results are shown and analysed in Section III. Finally, the modelling method is described in Section IV.

II. EXPERIMENTAL SET-UP

A. Device under test

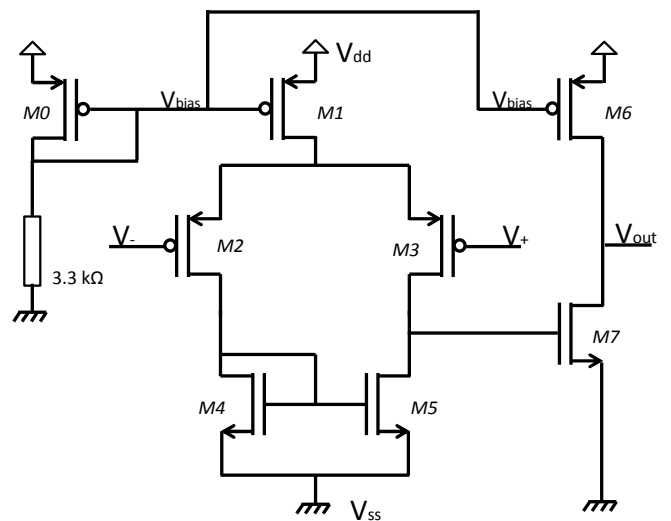


Fig. 1 Operational amplifier structure

The operational amplifier under test is embedded in a test chip designed in Freescale® CMOS 90-nm process. As illustrated in Fig. 1, it is a simple Miller operational amplifier. The bias voltage of the opamp is defined by an external resistor, and the output terminal (V_{out}) is an amplified copy of the voltage difference between the two input terminals (V_+ and V_-).

B. Electromagnetic susceptibility measurement

As described in Fig.2, the operational amplifier is in voltage-follower configuration, because this topology maximizes the susceptibility to EMI [7]. Normally, if there is no disturbance injected in the input terminal of a voltage-follower opamp, the output will track the input voltage (from 0.2 V to 3.1 V). The harmonic disturbances are produced by a RF signal synthesizer followed by a RF power amplifier, and they are superimposed to a constant voltage equal to 1.2 V and applied to the input of voltage-follower. The injected power is sensed with a directional coupler and a power meter. Both input and output voltage waveforms are observed with a 2 GHz digital storage oscilloscope equipped with 2.5 GHz active probes. The evolution of the EMI-induced DC offset on opamp output is measured according to the different EMI amplitude and frequency. The range of test frequency is from 10 MHz to 1 GHz.

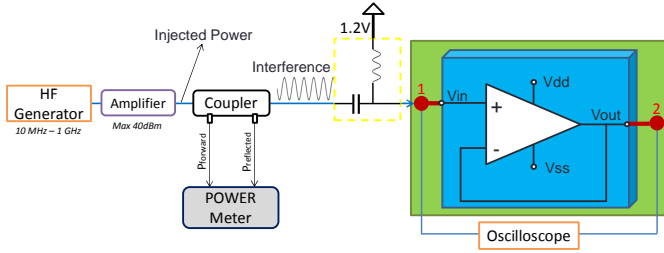


Fig. 2 Experimental setup for the susceptibility analysis of the amplifier

Besides, several key parameters of the amplifier are also measured, like the bias voltage/current and the positive slew rate (SR+) of the output voltage, which play an important role in the DC offset generation at low and middle frequencies [6].

C. Accelerated aging

The power supply voltage Vdd is risen to accelerate the aging of opamp. Two P-channel MOSFETs (M0 and M6 in Fig. 2) are the most affected by the aging stress. The aging condition is illustrated in Fig.3, the voltage stress is over the nominal functional voltage of the MOSFET of 3.3 V. Two components (component #1 and #2) are aged under 6 V, and one other (component #3) is aged by 5.5 V to observe the effect of different aging condition.

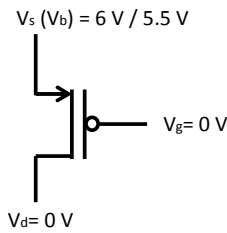


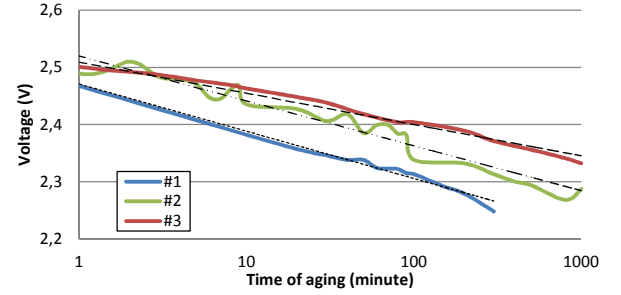
Fig. 3 Voltage stress on the transistor M0 and M6

The opamp are aged for 1000 minutes. The stress conditions are interrupted regularly (e.g. after 1 minute, 2 minutes, 5 minutes...) in order to measure the evolution of the opamp parameters and the output offset while the opamp operates under a nominal power supply of 3.3 V.

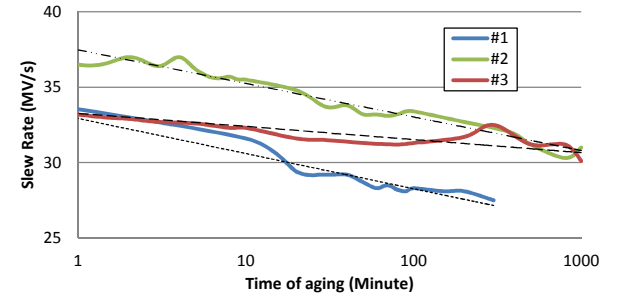
III. MEASUREMENT RESULTS

A. Evolution of parameters of opamp

The measured evolution of two parameters of the amplifier (bias voltage and positive slew rate) during the aging is presented in Fig. 4.



(a)



(b)

Fig. 4 Evolution of opamp parameters during the aging: (a) Bias voltage; (b) Positive slew rate (SR+) in the output

Though the parameters initial values of the devices are different because of the dispersion between the test chips, all these results reveal a decrease trend of both the bias voltage and positive slew rate (SR+) in the output after aging, as resumed in Table I. As the voltage stress of component #3 (5.5 V) is less than the other two devices (6 V), the parameters fall more steadily during the aging process according to the trend line equation.

TABLE I
EVOLUTION OF OPAMP PARAMETERS

Parameter	Com p. No	Stress Voltage	Initial value	Trend line (t is the aging time in minute)
Bias voltage (V)	#1	6 V	2.553	$y = -0.036 \ln(t) + 2.472$
	#2		2.577	$y = -0.035 \ln(t) + 2.525$
	#3	5.5 V	2.546	$y = -0.025 \ln(t) + 2.515$
SR+ (MV/s)	#1	6 V	35.3	$y = -0.991 \ln(t) + 32.84$
	#2		39.6	$y = -0.974 \ln(t) + 37.51$
	#3	5.5 V	35	$y = -0.307 \ln(t) + 32.96$

B. Evolution of electromagnetic susceptibility

Worse DC offsets are observed in the output during the aging for several chosen frequencies for all three test chips after aging. The results of device #3 are resumed in this section. As shown in Fig. 5, a gradual falling trend is observed during the aging process for all the EMI power range at only two EMI test frequencies of 10 MHz and 200 MHz, which

means that after aging the same EMI produces a larger DC offset in the output, or a less powerful EMI is sufficient to provoke the same DC output offset. In low frequency range (e.g. 10 MHz), these results could be explained by the decline of SR+ which is observed by the measurement, and in high frequency range the decrease offset after aging is related with the ascend of the bias current, which is caused by the descend of bias voltage V_{bias} [6].

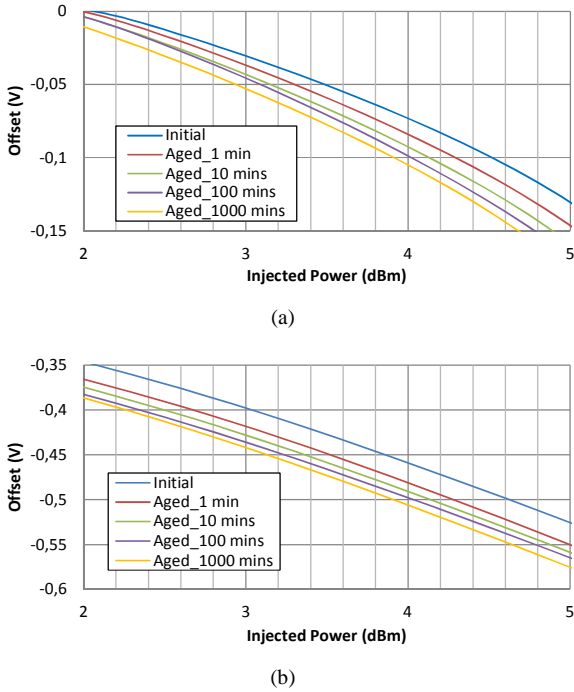


Fig. 5 Evolution of DC output offset during the aging process of different EMI frequency: (a) 10 MHz; (b) 200 MHz

The following immunity criterion is defined: the offset should not exceed ± 0.1 V. The evolution of susceptibility level of the opamp using this criterion is presented in Fig. 6. The component becomes more susceptible, except at 100 MHz. A gradual reduction of immunity level is revealed with increasing aging time at most test frequencies (except 50 MHz and 100 MHz).

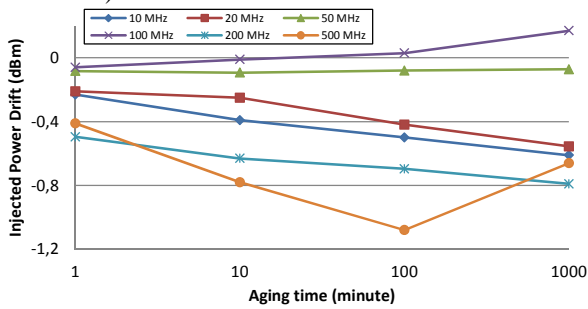


Fig. 6 Evolution of the immunity level at different EMI frequencies during the aging process

IV. LONG-TERM IMMUNITY PREDICTION

As presented in [4], the long-term immunity prediction model contains two parts: a model of the susceptibility of the circuit and a model which integrates the aging effect of

devices. All the simulations are based on SPICE and performed with Agilent's Advanced Design System (ADS).

A. Susceptibility model

The structure of the susceptibility model (Fig. 7) relies on ICIM standard proposal [8] which comprises two parts. Power Distribution Network (PDN) block describes the coupling path of the EMI to the injected nodes of the opamp (the package, interconnectors and coupling between pins). These elements are extracted by S-parameters measurements [9], and the modelling results fit well with the measurements at frequency range from 1 MHz to 500 MHz. Besides, Internal Behavior (IB) block models the operation of opamp and especially its reaction to electromagnetic disturbance. This block consists in the transistor netlist of the opamp.

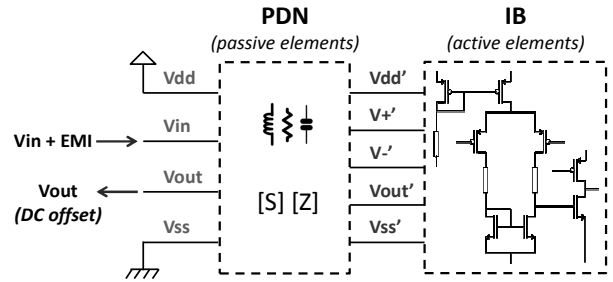


Fig. 7 Simplified susceptibility model of opamp

The previous immunity criterion is reused in the simulation. As shown in Fig. 8, a good correlation of the susceptibility level before aging is observed between the measurement and the simulation up to 500 MHz. Although the precision of the model at higher frequency is not perfect, it predicts the correct trends so we consider that it is satisfying for the integration of aging impact within the susceptibility model.

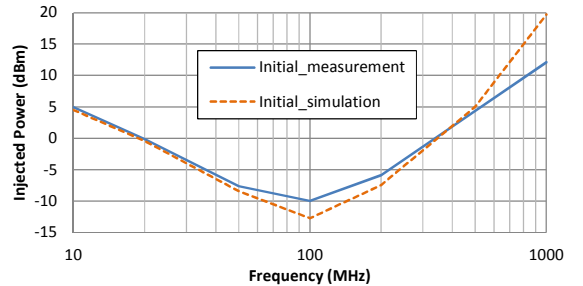


Fig. 8 Comparison between measured and simulated susceptibility level before aging

B. Aging effect model

The aging effect is included only in the IB block as the PDN measurements do not show any change after aging. The high drain-source and gate-source voltages of both P_channel MOSFETs accelerate degradation mechanisms such as Hot Carrier Injection (HCI) and Negative Bias Temperature Instability (NBTI) [10]. They result in the increase of threshold voltage, the decrease of mobility, trans-conductance and drain current. With the help of SPICE, the variation of threshold voltage shows a much more important role in the system behaviours than the others. So only the threshold voltage is set as the parameter which is affected by aging.

The threshold voltage of PMOSFET can be extracted by simulation from the measurement data of the bias voltage. The threshold voltage evolution with stress time is plotted in Fig. 9. As expected, the threshold voltage increases with stress time according to a power law dependence ($\Delta V_{th}(t) = A \cdot t^n$) [11]. Here the coefficient A is obviously related with the aging stress magnitude.

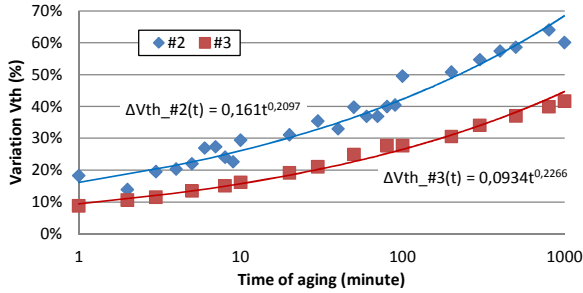


Fig. 9 Threshold voltage shift during the aging time

C. Long-term Susceptibility Simulation

The threshold voltage variation with stress time can be included in the transistor netlist so that the evolution of the susceptibility level according to the stress time can be simulated. The simulation results at 10 MHz and 200 MHz in Fig. 10 confirm not only the gradual increase of DC output offset at several frequencies during the aging, but also the offset level of different injected power.

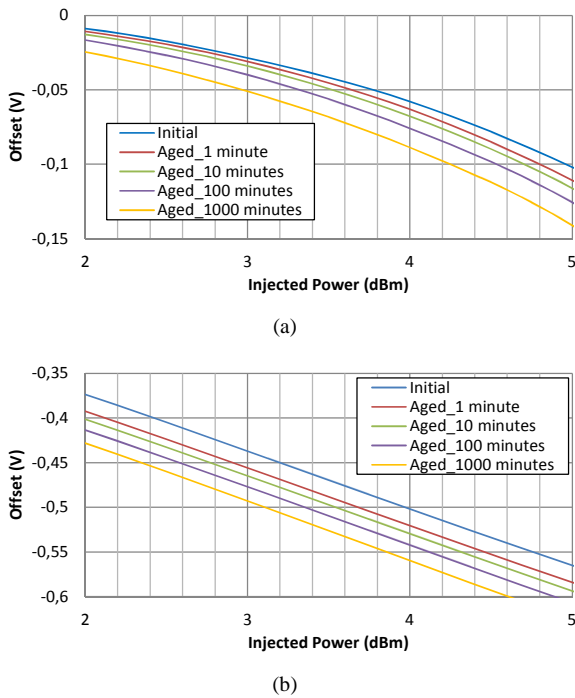


Fig. 10 Simulated evolution of DC output offset during the aging process of different EMI frequencies: (a) 10 MHz; (b) 200 MHz

As shown in Fig. 11, though the immunity drifts at 50 MHz and 100 MHz do not fit well with the simulation, the reduction of immunity level drifts during the aging process is found at most frequencies by the simulation.

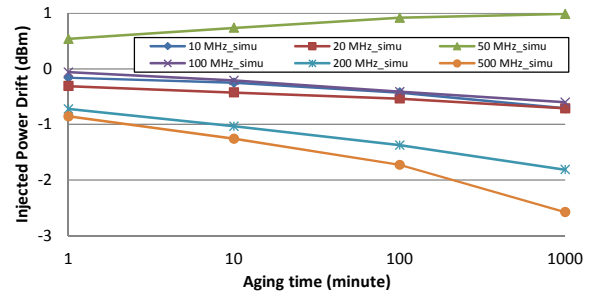


Fig. 11 Evolution of the immunity level at different EMI frequencies during the aging process by simulation

V. CONCLUSIONS

The aim of this paper is to find a practical method to predict the susceptibility level drift during IC aging. An operational amplifier is chosen for this study, and the devices are submitted to an electric stress aging. The experimental results show a gradual decrease of the immunity level. Based on the degradation mechanism analysis and the simulation comparison, the threshold voltage drift is chosen to present the aging impact. A long-term immunity prediction model is constructed, where the aging effect is included within the susceptibility model. Though the simulation results do not fit the measurement perfectly at every frequency, a global gradual reduction of immunity level is simulated correctly.

REFERENCES

- [1] S. Ben Dhia, M. Ramdani, E. Sicard, *Electromagnetic Compatibility of Integrated Circuits: Techniques for Low Emission and Susceptibility*, Springer, ISBN 0-387-26600-3, 2005.
- [2] S. Ben Dhia, A. Boyer, "Electro-Magnetic Robustness of Integrated Circuits: from statement to prediction", 9th International Workshop on electromagnetic Compatibility of Integrated Circuits, EMC Compo 2013, Dec. 15-18, 2013, Nara, Japan.
- [3] A. Boyer, H. Huang, S. Ben Dhia, "Impact of thermal aging on emission of a buck DC-DC converter", 2014 International Symposium on Electromagnetic compatibility, May 12-16, 2014, Tokyo, Japan.
- [4] A. Boyer, S. B. Dhia, B. Li, C. Lemoine and B. Vrignon "Prediction of long-term immunity of a phase-locked loop", Proc. IEEE 12th Latin-Amer. Test Workshop, pp.1-6, 2011.
- [5] F. Fiori, "A new nonlinear model of EMI-induced distortion phenomena in feedback CMOS operational amplifier," IEEE Trans. on EMC, vol. 44, no.4, pp. 521-527, Nov. 2002.
- [6] J.-M. Redouté, M. Steyaert, EMC of Analog Integrated Circuits, Springer, 2010.
- [7] G. Masetti, S. Graffi, D. Golzio, and Z. M. Kovcs-Vajna, "Failures induced on analog integrated circuits from conveyed electromagnetic interferences: A review", Microelectronics Reliability, vol. 36, no. 7/8, pp. 995972, 1996.
- [8] Marot C, Levant JL. Future IEC 62433-4: integrated circuit - EMC IC Modelling - Part 4: ICIM-CI, integrated circuit immunity model, conducted immunity. New Work Item Proposal, 2008.
- [9] J. Wu, A. Boyer, J. Li, B. Vrignon, S. Ben Dhia, E. Sicard, R. Shen, "Modeling and Simulation of LDO Voltage Regulator Susceptibility to Conducted EMI", IEEE Transactions on Electromagnetic Compatibility, Vol. 56, Issue: 3, pp 726 – 735, June 2014
- [10] V. Huard, C. R. Parthasarathy, A. Bravaix, T. Hugel, C. Guérin, E. Vincent, "Design-in reliability approach for NBTI and hot-carrier degradations in advanced nodes", IEEE Transactions on Device and Materials Reliability, Vol. 7, No. 4, December 2007.
- [11] B. Li, Study of aging effects on electromagnetic compatibility of integrated circuits. Thesis, University of Toulouse, 2011.